

### Force response to fast stretches applied at low tension in activated muscle fibres of the frog (*Rana esculenta*)

G. Cecchi, F. Colomo, B. Colombini, P. Geiger, R. Berlinguer Palmmini and M.A. Bagni

Dipartimento di Scienze Fisiologiche, Università degli Studi di Firenze, Viale G.B. Morgagni 63, I-50134, Firenze, Italy

We reported previously that the force transient produced by a fast stretch, applied to a skeletal muscle fibre during the early phases of a twitch contraction, was followed by a period, lasting several milliseconds, during which tension remained constant at a value well above isometric tension (Bagni *et al.* 1994). Such a maintained increase of force was not expected on the basis of cross-bridge kinetics, since reversal of the power stroke should quickly restore the original tension (in about 1 ms) by relieving the strain produced by the external stretch on series elasticity (Ford *et al.* 1977). This suggested to us that the excess tension, referred to as static tension, was not arising from stretched cross-bridges, but from some unknown elastic sarcomere structure whose stiffness (static stiffness) increased upon activation (Bagni *et al.* 1994). Several other observations were consistent with this hypothesis: static stiffness (1) started to increase during the latent period about 2–3 ms after the stimulus; (2) followed a time course clearly distinct from that of tension; (3) was practically unaltered when 1–3 mM of 2,3-butanedione monoxime (BDM) reduced twitch tension by more than 90%; (4) showed no correlation with myofilament overlap when sarcomere length was altered; (5) reached its value with no delay at the end of the stretch, even when stretch duration was too short to allow significant cross-bridge cycling. A complete analysis of the static stiffness properties under steady-state conditions was performed recently by studying the force responses to stretches applied during tetanic contractions (Bagni *et al.* 2002). In these experiments BDM at 1–8 mM concentration was added to the Ringer solution to inhibit tetanic tension (by as much as 98%). This reduced the number of attached cross-bridges and allowed isolation of the response of the static stiffness to stretch. In addition, unlike fully activated fibres, fibres in BDM were not damaged by the stretches and retained their sarcomere length homogeneity. Stretches of various amplitude (up to 40 nm  $\text{hs}^{-1}$ ) and duration (0.4–0.8 ms) were applied to the fibre at tetanus plateau and at different times after the start of stimulation. Static tension increased linearly with stretch amplitude in the whole range tested and was independent of stretch duration (up to 30 ms), as expected from a pure Hookean elastic response. As in twitches responses, static stiffness changed following the start of stimulation and was not correlated with tension. Static stiffness reached a peak about 10 ms after stimulation, when tension developed by the fibre was still very small, and it decayed within 100–200 ms to a constant level lasting until the start of relaxation. The mean stiffness measured at tetanus plateau in six fibres at a mean tension of 0.0360 ( $\pm 0.0038$  S.E.M.) times tetanic tension in normal Ringer ( $P_0$ ), was  $1.24 \times 10^{-3}$  ( $\pm 0.12 \times 10^{-3}$  S.E.M.)  $P_0$  (nm  $\text{hs}^{-1}$ ). This value corresponds to less than 1% of the total fibre stiffness measured at plateau in normal Ringer solution. Data from twitch contractions showed that static stiffness development followed a time course roughly similar to that of intracellular  $\text{Ca}^{2+}$  concentration, suggesting a possible correlation between the two parameters. This hypothesis has been tested by measuring static stiffness in the presence of various agents, such as Dantrolene, Methoxiverapamil (D600), and Ringer made with  $\text{D}_2\text{O}$ , which have all been shown to depress twitch tension mainly by reducing calcium release with no direct action on cross-bridge formation. Experiments were also performed in hypertonic Ringer (up to 1.6 normal tonicity). Similarly to BDM, hypertonic Ringer depressed twitch tension

without affecting calcium release. Data from five fibres showed that, relative to normal Ringer, hypertonic solution (1.4 T), reduced tension to  $0.270 (\pm 0.045 \text{ S.E.M.})$  while static stiffness was left practically unaltered (reduced to  $0.980 \pm 0.030 \text{ S.E.M.}$ ). On the contrary a similar twitch reduction ( $0.2 \pm 0.038 \text{ S.E.M.}$ ) produced by Dantrolene (at  $10 \mu\text{M}$  concentration) was accompanied by a substantial static stiffness reduction to 0.64 ( $\pm 0.0383 \text{ S.E.M.}$ ). In general, the results showed that static stiffness was almost unaffected by BDM and hypertonic solutions even when twitch tension was strongly inhibited. Twitch inhibition was instead accompanied by a static stiffness reduction when deuterium oxide or Dantrolene or D600 were added to the bath. These results suggest that static stiffness is modulated by intracellular calcium concentration.

Bagni, M.A. *et al.* (2002). *Biophys. J.* **82** (in the Press).

Bagni, M.A. *et al.* (1994). *J. Physiol.* **481**, 273–278.

Ford, L.E. *et al.* (1977). *J. Physiol.* **269**, 441–515.

All procedures accord with current UK legislation.

### Time-resolved X-ray studies of head domain orientation in the molecular motor, myosin, during force generation

P.J. Griffiths\*, M.A. Bagni†, B. Colombini†, H. Amenitsch‡, S. Bernstorff§, C.C. Ashley\* and G. Cecchi†

\*University Laboratory of Physiology, Parks Road, Oxford OX1 3PT, UK, †Dipartimento di Scienze Fisiologiche, Università di Firenze, V. Morgagni 63, Florence, I-50134, Italy, ‡Institute of Biophysics & X-Ray Structural Research, Austrian Academy of Science, Schmiedlstr. 6, A-8042 Graz Messendorf, Austria and §Sincrotrone Trieste, I-3401, Basovizza TS, Italy

Myosin molecular motors transduce free energy of ATP hydrolysis into work. Their proposed mechanism is rotation of the myosin S1 subfragment tail domain during S1 binding to actin. Proof of this rotation in a working myosin motor is crucial to acceptance of this mechanism. Uniquely, muscle myosin (myosin II) exists as highly structured filament aggregates of myosin dimers, from which three ‘crowns’ of S1 pairs project at axial intervals of 14.32 nm helically along the filament. In skeletal muscle, these filaments are parallel and radially aligned, giving rise to a quasi-crystalline structure which diffracts X-rays to produce a characteristic pattern. Time resolution of the muscle pattern intensity has increased dramatically in the past 40 years, from hours to microseconds, allowing use of X-ray diffraction as a time-resolved probe of S1 action.

The meridional reflection at 14.32 nm undergoes large intensity changes dependent on the occupancy of the ATP binding site and on the actin-bound S1 load. Its intensity ( $I_{M3}$ ) falls upon rapid stretch or release of a muscle. This fall is thought to result from an elastic tail domain angular displacement and a subsequent active, ‘power stroke’ tail rotation. However, in the case of a release,  $I_{M3}$  first passes through an intensity maximum ( $I_{M3,\text{max}}$ ), occurring when tail disposition produces the most concentrated S1 axial mass projection (Piazzesi *et al.* 1995).

We applied sinusoidal length changes (amplitude 5 nm per half sarcomere p-p, 100–3000 Hz, 4°C) to isolated muscle fibres (tibialis anterior from decapitated *Rana temporaria*) to examine the relation between  $I_{M3}$  and fibre length. At frequencies  $\geq 1$  kHz,  $I_{M3}$  signals were sinusoidal, in phase with sarcomere length with peak intensity at maximum shortening. As frequency was reduced below 1 kHz,  $I_{M3}$  signals became increasingly distorted, forming a new intensity minimum at maximum shortening,

causing a double  $I_{M3}$  peak about this point. Simulation of both tail domain displacement and  $I_{M3}$  showed that this behaviour was explicable as summation of elastic and active tail rotations: at  $\geq 1$  kHz, oscillations were fast compared with the power stroke, and  $I_{M3}$  arose chiefly from elastic motion of the tail; below 1 kHz, active tail displacement proceeded further, increasing total angular tail displacement and carrying it through its position at  $I_{M3,max}$  during shortening, thus forming a new intensity minimum at maximum shortening. At all frequencies, we found an axial shortening of  $< 0.9$  nm per half sarcomere was required to displace the tail domain to its  $I_{M3,max}$  position in our simulations (Bagni *et al.* 2001). Mean force during oscillations was  $\leq 5\%$  of isometric tension at all frequencies. Because distortion was absent at high frequencies, we could not determine tail disposition in this range, nor could we reject the possibility that the  $I_{M3}$  double peak depended on the presence of a power stroke component rather than on axial displacement. To test this, we used shorter fibres in which the applied oscillations caused a proportionally greater change in sarcomere length. We found a similar  $I_{M3}$  distortion to that at lower frequencies, in spite of a severely truncated active  $I_{M3}$  component (33% of tail motion at 200 Hz; 8% at 3 kHz; mean position 0.92 nm from  $I_{M3,max}$ ).

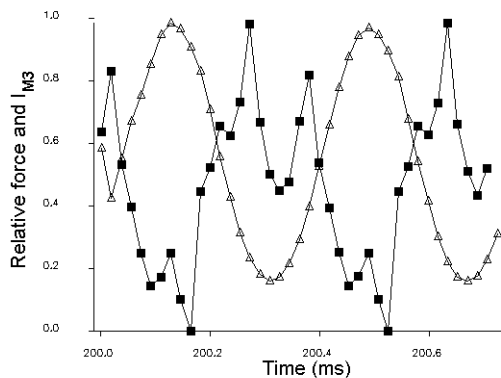


Figure 1. Relative force ( $\Delta$ ) and  $I_{M3}$  ( $\blacksquare$ ) during 3 kHz sinusoidal length oscillations.

To test our method, we used the finding that temperature elevation increases S1 force. According to the power stroke theory, this should displace the tail domain towards  $I_{M3,max}$ . As predicted, we found  $I_{M3}$  distortion increased as temperature rose, consistent with a 0.73 nm shift in tail mean position towards  $I_{M3,max}$  for a 28% increase in tension in our simulations. Simulations also showed that this effect was not accounted for by an increased power stroke contribution to  $I_{M3}$  at high temperature, or by changes in power stroke kinetics.

We conclude that, by use of the displacement required to reach an intensity reference point provided by  $I_{M3,max}$ , we have a complementary and independent method of determination of tail domain disposition to the Fourier synthesis determination of S1 structure by muscle fibre X-ray diffraction.

Bagni, M.A. *et al.* (2001). *Biophys. J.* **80**, 2809–2822.

Piazzesi, G. *et al.* (1995). *Biophys. J.* **68**, 92–98s.

This work was supported by EU Transnational Access contract HPRI-CT-1999-00033.

All procedures accord with current local guidelines.

## Myosin motor: functional diversity and molecular mechanisms

Roberto Bottinelli

*Institute of Human Physiology, University of Pavia, Via Forlanini 6, 27100 Pavia, Italy*

The basic contractile unit of striated muscle, the sarcomere, has a very high structural homogeneity. The basic mechanism of contraction appears the same for sarcomeric myosin (Myosin II) of all species. However, contractile and energetic properties of skeletal muscle fibres vary very widely from species to species and, within the same species, from muscle fibre to muscle fibre. In the last 20 years it has become clear that many myofibrillar proteins exist in several isoforms. Isoforms give to structurally homogeneous sarcomeres a large molecular heterogeneity both through species and within species. Investigations searching for the bases of the very high functional heterogeneity and plasticity of skeletal muscle have mostly focused on myosin heavy chain (MHC) isoforms.

MHC isoform function has been mainly studied by concomitant analysis of contractile and energetic properties and of MHC content of single skinned muscle fibres from small mammals and humans (Bottinelli & Reggiani, 2000). Single muscle fibres containing different MHC isoforms were found to have mostly different contractile and energetic properties with some relevant exception. Single muscle fibres containing MHC-I had 10-fold lower maximum shortening velocity ( $V_o$ ), maximum power, and rate of tension raise, and 3- to 4-fold lower optimal velocity, ATPase activity and tension cost than single muscle fibres containing MHC-IIB. MHC-IIA- and MHC-IIX-containing fibres had intermediate properties. Specific tension ( $Po/CSA$ ) and thermodynamic efficiency represent exception to the isoform based variability:  $Po/CSA$  was only 40% lower in MHC-I-containing fibres than in the other fibre types and thermodynamic efficiency was very similar in fibres containing different MHC isoforms.

Notwithstanding the progress in the understanding of skeletal muscle heterogeneity and plasticity, several open questions remain. It is still unclear whether MHC isoforms are the only determinant of skeletal muscle functional heterogeneity both within and through species. Moreover, very little is known about the mechanisms at the basis of functional diversity of skeletal myosin isoforms.

To clarify whether the differential expression of myosin isoforms can fully account for  $V_o$  differences among skeletal muscle fibres, *in vitro* motility assays (IVMA) were used to study the velocity of sliding of unregulated actin filaments ( $V_f$ ) on different MHC isoforms. In such IVMA any difference in the velocity of sliding of actin solely depends on the myosin isoforms loaded in the flow chamber. Sarcomere organization is in fact lost, all other myofibrillar proteins are absent, and actin is the same for all assays. With the aim to relate  $V_f$  of a given myosin isoform and  $V_o$  of the parent fibres over a large range of velocities and in several species, ten MHC isoforms from four species were analysed: mouse (MHC-I and -IIB), rat (MHC-I and -IIB), rabbit (MHC-I, -IIX and -IIB) and human (MHC-I, -IIA and -IIX). A linear relation was found between  $V_f$  and  $V_o$  through species. As in different species, myofibrillar protein isoforms and not only myosin isoforms are different, the results strongly support the view that variability in  $V_o$  among single fibres mostly depends on MHC isoform content.

The sequence of events in the acto-myosin cross-bridge cycle is thought to be the same for all myosin II forms. To generate different values of  $V_o$ , myosin isoforms might differ either in the amount of displacement determined by a single acto-myosin

interaction (step size) or in the kinetics of such interaction. To clarify whether the kinetics of acto-myosin interaction varies among myosin isoforms, acto-myosin interaction was studied in solution in a new flash-photolysis light-scattering apparatus (Weiss *et al.* 2001), developed in Mike Geeves's laboratory at the University of Canterbury, UK. Such apparatus enabled the analysis of the ATP-induced acto-myosin dissociation (apparent second-order rate constant,  $K_1k_{+2}$ ) on 1–2  $\mu\text{g}$  of myosin and of affinity of ADP for acto-myosin ( $K_{\text{AD}}$ ) on  $\sim 5 \mu\text{g}$  of myosin. The tiny amount of pure myosin isoforms required for analysis were obtained by extraction from single fibres. All four MHC isoforms from rat (MHC-I, -IIA, -IIX and -IIB) were studied. Consistently with the increase in  $V_o$  in the order type I, IIA, IIX, IIB fibres,  $K_1k_{+2}$  got faster whereas the affinity for ADP weakened ( $K_{\text{AD}}$  increased) in the isoform order I, IIA, IIX, IIB. Both  $K_1k_{+2}$  and  $K_{\text{AD}}$  linearly correlated with  $V_o$  of the parent fibres. Therefore, further analysis was required to identify which of the two parameters was rate-limiting of the whole process. The rate of ADP release ( $k_{-\text{AD}}$ ) was calculated from  $K_{\text{AD}}$  and compared with  $K_1k_{+2}$ . It was suggested that  $k_{-\text{AD}}$ , being 4- to 8-fold slower than  $K_1k_{+2}$ , is more likely to be the rate limiting step of  $V_o$ . To clarify whether differences in the rate of ADP release of myosin isoforms were sufficient to account for differences in  $V_o$  of single fibres, the minimum value of the rate constant of the event limiting shortening velocity ( $K_{\text{min}}$ ) was calculated for each fibre type from  $V_o$  values.  $k_{\text{min}}$  was determined according to Siemankowski *et al.* (1985) ( $k_{\text{min}} = V_o (\text{sarcomere length}) (\text{step size})^{-1}$ ).  $k_{\text{min}}$  agreed within a factor of 2 with  $k_{-\text{AD}}$ . The latter result confirms that  $k_{-\text{AD}}$  is the rate-limiting step of  $V_o$ , and strongly suggest that kinetics differences among skeletal myosin isoforms, namely a difference in ADP release rate, is the main determinant of  $V_o$  variability among skeletal muscle fibres.

Bottinelli, R. & Reggiani, C. (2000). *Prog. Biophys. Mol. Biol.* **73**, 195–262.

Siemankowski, R.F. *et al.* (1985). *Proc. Natl Acad. Sci. USA* **82**, 658–662.

Weiss, S. *et al.* (2001). *J. Biol. Chem.* **276**, 45902–45908.

*All procedures accord with current local guidelines and the Declaration of Helsinki.*

## Generating and sustaining human power output: the significance of muscle fibre type variability

Anthony J. Sargeant\*† and Arnold de Haan†

\*Centre for Clinical and Biophysical Research into Human Movement, Manchester Metropolitan University, Alsager, UK and

†Institute for Fundamental and Clinical Human Movement Science, Vrije University, Amsterdam, The Netherlands

In human locomotion the ability to generate and sustain mechanical power output is dependent on the organised variability in contractile and metabolic properties of the muscle fibres that comprise the active muscles.

In studies of maximum cycling exercise of short duration (10–25 s we used a microdissection technique to obtain fragments of single muscle fibres from needle biopsies before and after exercise. In this technique each fibre fragment was divided into two parts. One part was used to characterize the fibre type in respect of the heavy chain myosin isoform expressed. The other part of the fragment was used to determine high energy phosphate concentration (Sant'Ana Pereira *et al.* 1996; Karatzaferi *et al.* 2001). Fibres were classified on the basis of expressing either type I, type IIA, or type IIX myosin heavy chain isoforms. It should be noted, however, that in the type II

population many fibres co-expressed both IIA and the IIX isoforms and we therefore characterized these fibres on the basis of the degree of co-expression. Moreover, while there were significant numbers of fibres expressing only the IIA isoform very few fibres were seen in our normal healthy subjects which only expressed IIX.

We were able to show that immediately following 25 s of maximal effort exercise, during which mechanical power output declined by  $\sim 50\%$ , phosphocreatine (PCr) was reduced to zero, or near zero levels in all fibres. ATP was also reduced from 53 to 34 % of resting levels in the type II fibre subgroups, and to  $\sim 75\%$  in type I fibres, with a concomitant increase in IMP (Sant'Ana Pereira *et al.* 1996).

Subsequently we sought to explore the time course of this dramatic depletion in high energy phosphate using shorter duration cycling exercise ( $\sim 20$  contractions in 10 s; Karatzaferi *et al.* 2001). In these experiments maximum power output decreased by  $\sim 23\%$ . Fibre fragments were classified as either type I, IIA, IIAX or IIXa (the latter two classifications of co-expressing fibres having respectively a predominance of type IIA or IIX isoform). Immediately post-exercise PCr content in the four fibre populations decreased to 54, 47, 38 and 41 % of resting values. ATP showed no change in type I fibres but decreased to 75, 33 and 30 % of resting values in type IIA, IIAX and IIXa fibre groups. There was no detectable IMP in the type I fibres but significant IMP production in type II fibre populations despite the presence of PCr. The results suggest that maximal all-out exercise presented a sequential metabolic challenge to first the type IIX-expressing fibres, then IIA fibres and finally the type I fibres. It seems entirely reasonable that during maximal activation those fibre populations with the fastest cross-bridge cycling rates, as determined by myosin heavy chain isoform expressed, will deplete high energy phosphates at the greatest rate, resulting in selective fatigue of that population. Thus although the whole muscle mechanical output may decrease by only 25 % in 20 contractions this may obscure the fact that some fibre populations may be generating very little mechanical output while others will be relatively unaffected. The progressive reduction of power during maximal sprint efforts may be interpreted as the cumulative effect of metabolic depletion in successive fibre type populations from IIX to IIXa to IIAX to IIA to I.

This interpretation would be consistent with a previous observation that prior exercise (6 min at 90 %  $V_{O_{2\text{max}}}$ ) resulted in a decrease in maximum leg extension power that was velocity dependent. As the contraction velocity at which maximum power was measured increased, so did the magnitude of the fatigue. It was suggested that this was due to the selective fatigue of the fastest fatigue-sensitive fibres, which in a mixed muscle will contribute an increasing proportion of the maximum power output as velocity increases (Beelen & Sargeant, 1991).

Nevertheless, the relative contribution of different muscle fibre populations to mechanical output during whole body human movement of different intensities, types, and velocity remains a matter of some conjecture. Although one important future application of our microdissection technique is that PCr content may be used as a very sensitive metabolic marker for fibre type recruitment during very short duration exercise involving only a few contractions. In a recent communication to the Society we have shown that after even four contractions of the knee extensor muscles there are detectable changes in PCr content (Beltman *et al.* 2001).

There are considerable difficulties in relating the contraction velocity of isolated muscle preparations to human whole body exercise and quantifying the contribution of different fibre type populations to mechanical output. Nevertheless the issue is of considerable interest, having as it does an impact on choice of

movement cadence as it affects power output, mechanical efficiency, and strategies for improving muscle function including during, e.g. functional electrical stimulation and rehabilitation therapy. In a series of experiments since 1981 we have used cycling as an experimental model and believe that there is accumulating evidence to support the view that under normal conditions human type I fibres will be operating around their optimum for maximum power at a pedalling rate of about 60 rev min<sup>-1</sup>, with type IIA fibres, and those expressing increasing proportions of IIX myosin heavy chain isoform having optima at increasing pedalling speeds. Similarly we believe that the efficiency/velocity relationship can be placed in relation to whole body cycling exercise (Sargeant, 1999).

Beelen, A. & Sargeant, A.J. (1991). *J. Appl. Physiol.* **71**, 2332–2337.

Beltman, J.G.M. *et al.* (2001). *J. Physiol.* **533.P**, 128P.

Karatzafieri, C. *et al.* (2001). *Exp. Physiol.* **86**, 411–415.

Sant'Ana Pereira, J.A.A. *et al.* (1996). *J. Physiol.* **496**, 583–588.

Sargeant A.J. (1999). *Physiological Determinants of Exercise Tolerance in Humans*, ed. Whipp, B.J. & Sargeant, A.J., pp. 13–28. Portland Press/Physiological Society.

*All procedures accord with current local guidelines and the Declaration of Helsinki.*

## Between muscles and movement: tendons and their properties *in vivo*

Constantinos N. Maganaris

*Centre for Biophysical and Clinical Research into Human Movement, Manchester Metropolitan University, Hassall Road, Alsager ST7 2HL, UK*

Contractile forces are transmitted to the skeleton through tendons. Numerous *in vitro* studies have shown that although tendons are stiff enough to act as effective force transmitters, they exhibit a time-dependent behaviour (e.g. Bennett *et al.* 1986). However, relying exclusively on results from experiments on isolated specimens when seeking to interpret physiological function may be inappropriate because *in vitro* testing necessitates application of conditions that deviate largely from the physiological environment of tendon. For example, the clamps used in *in vitro* testing may allow specimen slippage and artifactual elongations. Moreover, in contrast to physiological conditions, a specimen under *in vitro* conditions is biologically inert and is often tested after preservation and storage, which may alter the properties of the material.

We recently developed a method for *in vivo* quantification of the load-elongation response of human tendon (Maganaris & Paul, 1999, 2000). In this method, tendon loads are generated by contraction of the in-series muscle, and the resultant tendon elongations are taken from ultrasound-based measurements of the displacement of an anatomical landmark in the tendon proximal end. To avoid displacements in the tendon bony attachment, the contractions are elicited isometrically. The muscle moments generated by contraction are quantified using dynamometry, reduced to tendon forces using information about moment arm lengths obtained from analysis of magnetic resonance images (MRIs), and then combined with the respective tendon elongations to obtain the tendon force-elongation relation. Reduction of the force-elongation relation to the dimensions of the tendon, obtained again from analysis of MRIs, yields the stress-strain relation of the tendon.

We applied the above principles to examine the mechanical behaviour of the highly stressed and spring-like acting human gastrocnemius (GS) tendon, and the less highly stressed human tibialis anterior (TA) tendon. Our results from measurements in six healthy volunteers showed that, at forces corresponding to the maximal isometric muscle force, either tendon has a Young's modulus of ~1.2 GPa, which is in line with *in vitro* results (Bennett *et al.* 1986) and suggests that the material of tendon does not adapt to produce a stiffer or more compliant structure in response to differences in the physiological loading applied. The mechanical hysteresis of either tendon was found to be ~19%, which is larger than the average value of ~10% reported from *in vitro* tests (Bennett *et al.* 1986), indicating that in our *in vivo* method heat loss from sources other than the tendon occurs, e.g. in the myotendinous and osteotendinous junctions and due to surface friction between the tendon and its surrounding tissues. In the GS tendon, the heat loss levels found could implicate the development of hyperthermia due to the high and repeated loading applied, predisposing the tendon to mechanical failure.

A second series of experiments were carried out to quantify the extent to which *in vivo* tendons exhibit force relaxation, i.e. a decrease over time in the force required to produce a given elongation. The experiments were performed in the human GS tendons of six healthy volunteers performing repeated isometric plantarflexion contractions-relaxations. Our results showed that the plantarflexion moment required to produce tendon elongations of 7 and 11 mm (7 mm corresponds to the tendon elongation during slow walking, Fukunaga *et al.* 2001; 11 mm corresponded to 90% of the maximal elongation in the experiments) decreases by ~17% in five consecutive contraction-relaxation cycles, following a curvilinear pattern as a function of cycle number. The relaxation found is in line with experiments from previously unloaded, 'unconditioned' tendons (Haut & Powlison, 1990), indicating that 'conditioning' is a relevant property of tendon and not a clamping-induced artifact.

The relaxation of *in vivo* tendon would allow the in-series muscle to shorten more as a function of cycle number and therefore reduce its fascicular length and increase its pennation angle, a hypothesis tested in a separate experiment. Indeed, repeated plantarflexion contractions at 80% of the maximal plantarflexion moment altered the fascicular length and pennation angle as predicted, following the force relaxation pattern of the in-series tendon. The total reduction in fascicular length was ~12%, which according to the cross-bridge mechanism of contraction would reduce the force-generating potential of the muscle by ~5% compared with the first contraction. The total increase in pennation angle was ~20%, which according to a simple planimetric muscle-tendon model would decrease the maximal plantarflexion moment produced by ~10% compared with the first contraction.

To conclude, our results indicate that *in vivo* tendons do not behave as rigid structures, but exhibit viscoelastic properties as those seen when testing *in vitro* material. These findings have functional implications for contractile force generation and joint movement.

Bennett, B.M. *et al.* (1986). *J. Zool. Lond. A* **209**, 537–548.

Fukunaga, T. *et al.* (2001). *Proc. R. Soc. Lond. B* **268**, 229–233.

Haut, R.C. & Powlison, C. (1990). *J. Orthop. Res.* **8**, 532–540.

Maganaris, C.N. & Paul, J.P. (1999). *J. Physiol.* **521**, 307–313.

Maganaris, C.N. & Paul, J.P. (2000). *J. Biomech.* **33**, 1723–1727.

*All procedures accord with the Declaration of Helsinki.*

## Of sprint running or running uphill?

P.E. di Prampero, S. Fusi and G. Antonutto

Dipartimento di Scienze e Tecnologie biomediche, Università degli Studi di Udine, p. le Kolbe 4, 33100 Udine, Italy

The speed of the initial 20 m of an all-out run from a stationary start on a flat track was continuously determined on eight medium level sprinters (3 females and 5 males) by means of a wire tachometer. The wire was attached to a belt placed approximately at the centre of mass. The running speed increased to a peak of  $8.48 \text{ m s}^{-1}$  (0.33 s.d.) in females ( $n = 9$ ) and to  $9.31 \text{ m s}^{-1}$  (0.31) in males ( $n = 29$ ) after 3.07 s (0.085) and 2.82 s (0.09) from the start, respectively. The highest forward acceleration ( $a_f$ ) was observed immediately after the start (0.25 s): it was  $4.75 \text{ m s}^{-2}$  (0.13) in females and  $5.77 \text{ m s}^{-2}$  (0.25) in males.

In the acceleration phase, the runner leans forward by an amount that depends on  $a_f$ . The angle by which the runner leans forward can be calculated assuming that the average force ( $F$ ) during the stride cycle is applied along a line joining the centre of mass and the point of contact foot-ground. If this is so, the angle  $\alpha$  between the runner's body (assumed to coincide with the direction of  $F$ ) and the terrain is given by  $\alpha = \arctan g/a_f$  (see Fig. 1). The angle  $\alpha$  could then be calculated, allowing us to determine the 'equivalent slope' (ES). This is defined as the incline of the terrain, in respect to the horizontal, which would allow the runner, if running at constant speed, to maintain a vertical body position. The equivalent slope is given by:  $\text{ES (deg)} = 90 - \alpha$  (see Fig. 1). It was shown that ES reached a maximum of 25.9 deg (0.63) (48.6%) in females and 30.5 deg (1.1) (58.9%) in males, attained at the time coinciding with the highest values of  $a_f$ . Thereafter, ES decreased to a value equal to or lower than 5% after about 3 s. It should also be pointed out that ES, as calculated, refers to the value in excess of that corresponding to running at constant speed on flat terrain, in which case the runner lies slightly forward. The maximal average vertical force during the stride cycle, as given by the product of the vectorial sum of  $a_f$  and  $g$  and the subject's body mass ( $F = \text{BM} (g^2 + a_f^2)^{0.5}$ , see Fig. 1), was also calculated: it was about 1.11 and 1.16 times the body weight in females and males, respectively. ES and  $F$  allowed us to calculate the energy cost of sprint running ( $C_{\text{sr}}$ ) from the data recently obtained by Minetti *et al.* (2002) during uphill running, up to a maximum incline of 45%. The peak  $C_{\text{sr}}$ , coinciding with the highest value of  $a_f$  was 20.0 and 24.9 J (kg m) $^{-1}$ , in females and males; the average, integrated over the 20 m corresponding to the acceleration phase, was 10.1 and 13.3 J (kg m) $^{-1}$ , to be compared with 3.8 J (kg m) $^{-1}$  for running at constant speed on flat terrain.

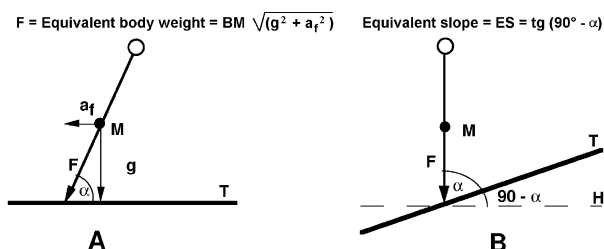


Figure 1. The subject is accelerating forward while running on flat terrain (A) or running uphill at constant speed (B). Forward acceleration ( $a_f$ ), acceleration of gravity ( $g$ ) and their vectorial sum ( $F$ ) are assumed to be applied at the centre of mass of the subject ( $M$ );  $F (= \text{body mass} (g^2 + a_f^2)^{0.5})$  is the average force throughout the stride cycle; T = terrain; H = horizontal;  $\alpha (= \arctan g/a_f)$  is the angle between

runner's body and T;  $90 - \alpha$  is the angle between T and H, the tangent of which yields the equivalent slope ES.

It is concluded that the present approach yields a fruitful estimate of the energy cost of sprint running.

Minetti, A. *et al.* (2002). *J. Appl. Physiol.* (in the Press).

All procedures accord with current UK legislation.

## The biomechanical determinants of increased speed in passively assisted human-powered locomotion

Alberto E. Minetti

Centre for Biophysical and Clinical Research into Human Movement, Manchester Metropolitan University, Alsager ST7 2HL, UK

The endeavour for exploration and the innate curiosity pushed humans to adapt locomotion to different environments, despite the inherent limits in body anatomy and physiology. This process, confined today to leisure because of the availability of active machines, started a couple of millennia ago and benefited from passive locomotor tools. The tools can be grouped into terrestrial, aquatic and aerial categories, with the common feature of enhancing muscle performance to achieve a higher mechanical power, economy, sustainable speed and/or distance range.

The first tools devoted to increase the human performance in the standing long jump were HALTERES, hand-held loads (1.2–4.5 kg) introduced in ancient Olympics pentathlon events (500–300 BC). Their role was: (a) to produce a higher ground reaction force by a more efficient use of shoulder extensor muscles, and (b) to alter the position of the body centre of mass (BCOM) at take-off (more anterior) and landing (more posterior). There are clues (Minetti, 2002) that these effects increased the jump range.

While studying the ability of our musculo-skeletal system to store and return elastic energy, Tom McMahon (1979) designed a purposely 'TUNED' TRACK where the surface stiffness was controlled and athletes were able to run faster.

However, running speed is limited by the constraint imposed by foot contact with the ground, which forces the lower limbs to be moved, with respect to BCOM, at the same speed the BCOM moves with respect to the environment. At that (increasing) speed, muscles operate (both for relocation and pushing) in a disadvantageous range of the force/velocity diagram. The invention of skating, in all its forms, partially solves this problem by allowing the appendages to move and push at a slower, more efficient, speed. ICE/IN-LINE SKATING (3000 BC–ca 1980), also used for transportation on the iced Amsterdam canals (about 14th century), is in its modern form the fastest non-wheeled human-powered locomotion (very low friction: 0.003–0.007). The lateral push while sliding allows knee and ankle extensor muscles to operate within the optimal contraction speed range. The reduced added mass and speed of limbs with respect to BCOM also implies a low mechanical internal work ( $W_{\text{INT}}$ , i.e. the work necessary to accelerate body segment with respect to BCOM). The modern roller in-line skating, while being slower because of the higher rolling resistance, benefits from the same physiomechanical strategy of ice skating. Another success of the skating protocol can be found in CROSS-COUNTRY SKI (2000 BC–1980). Originally a means of travel and communication in Scandinavia and Russia, it is today the second fastest non-wheeled locomotion because of the very low friction (0.05–0.20) and the small added mass involved. Skating

is the fastest technique, which adopted the ice-skating strategy for lower limbs (lowering  $W_{\text{INT}}$  and increasing muscle efficiency) and made a better use of 'energy recovery', i.e. the exchange between the potential and kinetic energy of BCOM (Cavagna *et al.* 1976), and the related mechanical external work ( $W_{\text{EXT}}$ , Minetti *et al.* 2001a). The other available techniques, namely the diagonal stride and the double pole, are slower mainly because the propulsion is achieved by the push on the snow of skis and poles, which stop with respect to the ground, with the above explained detrimental effects on  $W_{\text{INT}}$  and the muscle efficiency.

A great advancement in terrestrial human-powered locomotion has been achieved when the wheel helped to sustain the BCOM, thus avoiding spending metabolic energy to counteract gravity, both isometrically and during the typical vertical oscillations as occurring in walking/running/skating. The idea behind the BICYCLE (1820–) was an alteration of body geometry in order to escape from the rimless wheel metaphor of legged locomotion. By preventing the vertical displacements of BCOM, the lower limb muscles can be used mainly to overcome rolling resistance and air drag. By progressing from the Hobby Horse (1820), where the rider pushed directly on the ground, to the High Wheeler (1870) and the modern bicycle (1890), the metabolically equivalent cruising speed, with respect to walking ( $1.5 \text{ m s}^{-1}$ ), increased 3.3 times ( $\sim 5.0 \text{ m s}^{-1}$ , Minetti *et al.* 2001b). The major determinants of locomotor economy improvement in cycling evolution were: (1) the decrease of the overall bicycle mass (from 24 to 16 kg), which helped to further decrease (2) the decreased rolling resistance (0.027 to 0.008), due to the transition from metal to solid and inflatable tyres, (3) the concurrent lengthening of the distance travelled per pedal revolution (2.8 to 5.5 m), which caused (4) the decrease of pedalling rate (fr) at a given speed and, consequently, (5) the decrease of  $W_{\text{INT}}$  (which in cycling depends on  $\text{fr}^3$ ). In addition, the last two effects maximized the efficiency of knee extensor muscles at high progression speed, allowing them to keep on contracting within the optimal speed range. The modern racing bicycle is the fastest human-powered vehicle available.

Aquatic locomotion benefited by appendages for hands and feet devoted to improve propulsion. With respect to normal kick swimming FIN SWIMMING (fin pairs 1680–1935, monofin 1967) decreases the metabolic cost by about 40%, allowing  $0.2 \text{ m s}^{-1}$  speed increase. It has been found that  $W_{\text{INT}}$  and the kinetic energy imparted to the amount of water not involved in propulsion decrease by using fins, thus the Froude efficiency and the hydraulic efficiency increase, respectively (Zamparo *et al.* 2002).

In conclusion, the increase of economy/cruising speed (or of jumping range) has been obtained by each of the illustrated passive appendices throughout a combination of the following strategies: (a) the decrease of  $W_{\text{EXT}}$ , (b) the decrease of  $W_{\text{INT}}$ , (c) the modification of body configuration, devoted to retain muscle performance optimization.

Cavagna, G.A. *et al.* (1976). *J. Physiol.* **262**, 639–657.

McMahon, T.A. *et al.* (1978). *Scientific American* **239**, 148–163.

Minetti, A.E. *et al.* (2001a). In *Science and Skiing II*, ed. Müller, E. *et al.*, pp. 30–42. Hamburg, Kovac.

Minetti, A.E. *et al.* (2001b). *Proc. R. Soc. B* **268**, 1351–1360.

Minetti, A.E. (2002). *7th ECSS Congress*.

Zamparo *et al.* (2002). (submitted).

*All procedures accord with current local guidelines and the Declaration of Helsinki.*